Journal of Chromatography, 255 (1983) 359–379
Elsevier Scientific Publishing Company, Amsterdam — Printed in The Netherlands

CHROM. 15,365

CAPILLARY LIQUID CHROMATOGRAPHY IN FIELD FLOW FRACTIONATION-TYPE CHANNELS*

J. C. GIDDINGS*, J. P. CHANG**, M. N. MYERS, J. M. DAVIS and K. D. CALDWELL
Department of Chemistry, University of Utah, Salt Lake City, UT 84112 (U.S.A.)

SUMMARY

Recent attention has focused on the potential of using open capillary tubes for liquid chromatography. These tubular columns are confronted by two intensely conflicting demands: tube diameter (d_c) must be extremely small to facilitate rapid mass transfer and thus rapid analysis, and the tube diameter must be relatively large to accommodate sample handling and detection while maintaining high resolution. This conflict can be largely resolved by using a column of ribbon-like instead of thread-like bore. Such "ribbon" columns, or, more technically, open parallel plate columns (OPPC), have two adjustable cross-sectional dimensions with which to resolve the two conflicting demands. The thickness (w) of the channel can be made extremely small for rapid mass transfer, and the breadth can be made relatively large to increase column volume.

In this study, we have developed theoretical expressions for the comparison of OPPC and open capillary tube systems. The comparison of such parameters as surface area per unit volume, plate height, speed, and permeability shows that the two columns are roughly comparable for equal dimensions ($d_c = w$). However, a comparison based on the theory of Knox and Gilbert, which requires that columns be compatible with the dead volume of available detectors, shows that OPPC systems have a potential analysis speed advantage ranging from about 100- to 300-fold.

We have constructed OPPCs based on the field flow fractionation design with gap thickness w of 100 μm, 78 μm, 56 μm, and 13 μm. Plate height *versus* velocity plots have been compared with theory. The 13-μm channel, with octadecylsilane coated on glass, provided the separation of a five-component mixture (sodium benzoate, benzene, naphthalene, biphenyl, and anthracene) in 10 min.

INTRODUCTION

Considerable attention has focused recently on the possibility that effective liquid chromatography (LC) can be carried out in capillary or open tubular col-

* *Editor's Note:* It is at the express wish of the authors that abbreviations are used throughout the text. *Editor J. Chromatogr.*

** Present address: Shanghai Institute of Materia Medica, Chinese Academy of Sciences, Shanghai, China.

0021-9673/83/0000–0000/$03.00

umns[1–4]. In order to achieve rapid mass transfer, such columns must be inordinately narrow, perhaps 5–25 μm in internal diameter. These columns have an internal volume of only 0.02 to 0.5 μl per meter of length. One of the disadvantages of the capillary LC approach is that these thin columns have such small volumes that it becomes very difficult to inject and detect samples without a great deal of incremental band spreading.

In order to retain the favorable characteristics of an open tubular column (OTC) without suffering the disadvantages of such extremely low volumes, we have developed an open parallel plate column (OPPC) in which a ribbon-shaped channel replaces the thread-like bore of OTCs. The OPPC design is patterned after field flow fractionation (FFF) channels, which we have developed extensively in our laboratory[5–7]. A schematic comparison of OTC and OPPC geometries is shown in Fig. 1.

The versatility of the FFF-based OPPC system would be extraordinary. Such OPPCs could be opened up for inspection and modification of the column wall and active surface. Special film-like inserts could be sandwiched between the original walls and the channel-forming spacer to generate new surfaces with any desired physical or chemical properties. These flat inserts, prepared outside the column using almost any desired material, would be much easier to modify and control in accordance with desired specifications than the inside walls of a closed capillary tube. The insert concept would allow one to develop separately and flexibly the structural component of the column, which assures the desired geometry and dimensions, and the surface component which is determined by the physically distinct insert.

The spacing between the flat faces forming an OPPC must be very narrow to encourage rapid mass transfer, in the same way that an OTC bore must be very small. At comparable dimensions, the two columns will act comparably (but not identically) with respect to mass transfer, pneumatic resistance, and surface (coating) area per unit volume of mobile phase. However, the volume of the OPPC system per unit length of column is much greater than that of the comparable OTC, roughly in proportion to the aspect ratio —the ratio of the breadth (side-to-side distance) to the thickness. Aspect ratios of *ca.* 1000 or more should be practical.

The geometrical advantages of an OPPC system can be summarized by noting that it provides two dimensions (thickness and breadth) for optimization. In theory

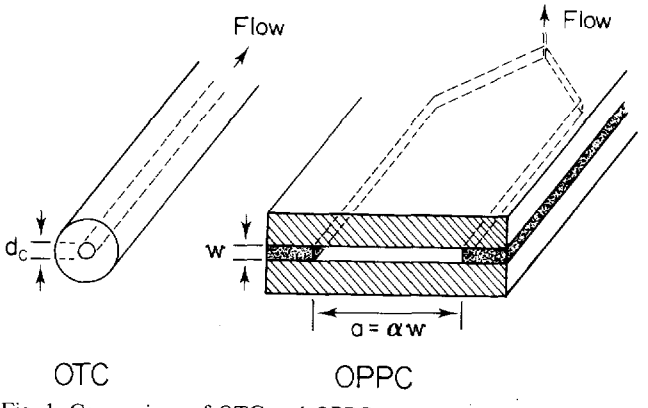

Fig. 1. Comparison of OTC and OPPC geometries for capillary LC. The breadth to thickness ratio (or aspect ratio) α may exceed 10^3.

the thickness can be reduced as much as necessary to ensure rapid mass transfer while the breadth can be increased to provide the necessary column volume and capacity.

We note that most FFF channels are 30 to 100 cm long, a length that should be adequate also for OPPC chromatographic systems. However, greater lengths could be achieved if desired through a hairpin configuration[8] or by means of coiling.

The comparison of requirements for OPPCs and FFF channels is interesting. The surfaces of FFF channels must be designed for inertness (since FFF is a one phase separation system), particularly so considering the interactive nature of the macromolecular and particulate species to which FFF is applicable. OPPCs, by contrast, must have surfaces designed for specific categories of physical and chemical activity. The two requirements are perhaps equally challenging: true inertness is a goal as elusive for complex macromolecules as is the achievement of general selectivity between all of the simple components of a complex mixture.

Contrary to what one might expect, the geometrical requirements of OPPCs will be more stringent than those for FFF columns. Both channel systems must be thin to avoid large mass transfer effects, but the FFF system has the advantage that the field-induced formation of narrow solute layers reduces the time for mass transfer several orders of magnitude below that existing when molecules have to diffuse across the entire channel thickness. Thus channels can be designed in the 50–250 μm range without any adverse effects, despite the inherently sluggish mass transfer properties of macromolecules and colloids. However, OPPCs, in which no layer formation occurs, will undoubtedly need to have a thickness considerably less than 50 μm, corresponding roughly to the diameter requirements of a viable OTC. It is increasingly difficult to maintain the geometrical integrity necessary for flow uniformity in channels of decreasing thickness. However, our success with FFF channels down about to 50 μm[9] suggests that the next level of reduction can be achieved without undue effort.

COMPARISON OF OPPCs AND OTCs

Volumetric considerations

The relevant dimensions of the OPPC system, labeled in accord with FFF terminology, are column thickness (or width), w, breadth, a, and length, L. OTCs have inner diameter, d_c, and length, L.

The respective cross sectional areas of OPPC and OTC systems (equal to the volume per unit of length) are

$$A(\text{OPPC}) = aw = \alpha w^2 \tag{1}$$

$$A(\text{OTC}) = \pi d_c^2/4 \tag{2}$$

where α is the aspect ratio, a/w. The ratio of areas (volumes) is

$$A(\text{OPPC})/A(\text{OTC}) = \frac{4\alpha}{\pi}\frac{w^2}{d_c^2} \tag{3}$$

When w and d_c are equal, so as to yield comparable mass transfer effects (see later), the area ratio becomes simply $4\alpha/\pi$. For an aspect ratio of $\alpha = 1000$, the volumetric advantage of the OPPC is consequently almost 1200-fold.

This volumetric advantage has perhaps its greatest significance in ameliorating the stringent low volume requirement for detectors in capillary LC. Knox and Gilbert[10] have indicated that the detector cell volume, V_c, should not exceed one-half of the standard deviation of a peak in volume units, σ_v, emerging from a capillary column, $V_c \leqslant \frac{1}{2}\sigma_v$. Assuming some minimum feasible detector cell volume, the ratio of retention volume, V_r, to cell volume must be governed by

$$V_r/V_c \geqslant 2N^{1/2} \tag{4}$$

where N is the number of theoretical plates. For effective capillaries, which for OTCs have internal volumes generally less than 1 μl/m, it is difficult to "generate" sufficient retention to satisfy the above criterion. Some of the compromises necessary to conform to eqn. 4 can be seen it we break V_r into its components

$$V_r = V^0(1 + k') = V^0(1 + K'S/V) \tag{5}$$

where V^0 is the column volume, k' is the capacity factor, K' is the equilibrium distribution ratio representing the number of molecules accumulated in the stationary phase for each unit area of surface divided by the number in a unit volume of mobile phase, and S/V is the surface area/column volume ratio. If we take S as the geometrical surface area (which is correct as long as we define K' in reference to unit geometrical area), the ratios S/V assume the form

$$S/V = 2/w \tag{6}$$

$$S/V = 4/d_c \tag{7}$$

for OPPCs and OTCs, respectively.

For an OTC, the substitution of eqn. 7 into eqn. 5 and the use of $V^0 = \pi d_c^2 L/4$ yield

$$V_r = \tfrac{1}{4}\pi d_c^2 L(1 + 4K'/d_c) \tag{8}$$

In order to reach the general goal expressed by eqn. 4, d_c and L must be increased beyond chromatographically optimal values. However, increasing d_c has a counterbalancing effect via the last term $4K'/d_c$, in the parentheses of eqn. 8. Furthermore, unduly decreasing $k' = 4K'/d_c$ leads to an erosion of resolving power, leading to even further departures from optimal performance. In theory K' can be increased to offset gains in d_c —perhaps by employing a support-coated open tubular column— but this can lead to further compromises. In sum, even assuming no k' problem, Knox and Gilbert[10] have shown that the compromises forced on the system by detector volume considerations lead to a wide departure from chromatographically optimized systems.

The retention volume of an OPPC is described by substituting $V^0 = \alpha w^2 L$ and eqn. 6 into eqn. 5.

$$V_r = \alpha w^2 L(1 + 2K'/w) \tag{9}$$

While the same general principles apply to this equation as to eqn. 8, the presence of aspect ratio α (perhaps 10^3 in magnitude) relaxes the harsh compromises required for dimensions w and L. Thus practical w and L values for OPPCs should be closer to chromatographically optimal levels than the corresponding d_c and L values of OTCs. This matter will be more thoroughly explored following an analysis of the performance characteristics of OPPCs and a comparison of OPPCs and OTCs when $w = d_c$.

Relative column performance

The plate height term that is most involved in establishing the ultimate limit to the speed of chromatographic separation is the non-equilibrium or mass transfer term. In capillary LC subject to normal laminar flow the irreducible minimum non-equilibrium contribution is that originating in the mobile phase. This contribution assumes the form

$$H = C_m\langle v\rangle \tag{10}$$

where C_m is the non-equilibrium coefficient and $\langle v\rangle$ is the mean mobile phase velocity. For the OPPC system, C_m is expressed most simply in terms of retention ratio, R (ref. 11)

$$C_m = (35R^2 - 84R + 51)w^2/210D_m = f_p(R)w^2/D_m \tag{11}$$

where R, equal to $1/(1 + k')$, is the ratio of the retention time of the void peak to that of the retained peak. Parameter D_m is the mobile phase diffusion coefficient.

For the OTC we use the following expression, equivalent to the Golay mass transfer term but again expressed in R rather than k' for simplicity[12]

$$C_m = (6R^2 - 16R + 11)d_c^2/96D_m = f_t(R)d_c^2/D_m \tag{12}$$

We will use the two expressions above for the comparison of OPPCs and OTCs. Subscripts p and t will represent OPPCs and OTCs, respectively.

We will assume for simplicity that we are working at flow-rates well in excess of the velocity optimum so that the plate height is described by eqn. 10. In this case the relative plate heights are obtained by substituting eqns. 11 and 12 into eqn. 10. At equal linear flow velocities, retention ratios, and diffusivities the ratio of plate heights becomes simply

$$\frac{H_p}{H_t} = \frac{f_p(R)w^2}{f_t(R)d_c^2} = \kappa\frac{w^2}{d_c^2} \tag{13}$$

The expression for the time required to generate N theoretical plates, $t = NH/R\langle v\rangle$, which approaches NC_m/R at high flow velocities[11], yields the following time ratio for the two techniques

$$\frac{t_p}{t_t} = \kappa\frac{w^2}{d_c^2} \tag{14}$$

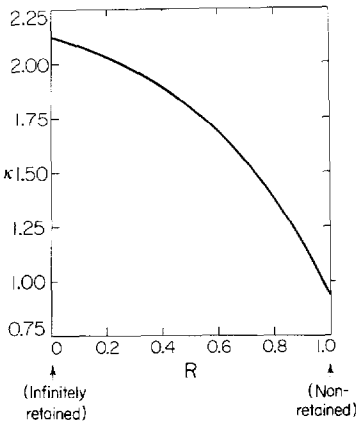

Fig. 2. Plot of κ *versus* R (see eqn. 13).

When the OPPC and OTC systems have the same critical dimensions, $w = d_c$, and are operated at the same level of retention as measured by R or k', the plate height and time ratios of the last two equations reduce to κ. Because of the importance of κ in the comparison of OPPCs and OTCs, we show a plot of κ *versus* R in Fig. 2. This figure shows that κ is approximately equal to two for moderate to high retention levels, $R < 0.5$. Thus OPPCs and OTCs will provide comparable plate height and speed providing $w \approx d_c/\sqrt{2} \approx 0.7d_c$. The reason w needs to be slightly smaller than d_c is clear on physical grounds: mass transfer from the center to the wall regions of a column is facilitated by the better accessibility of the totally encircling wall of the OTC.

Resistance to flow is another important measure of column effectiveness. For the laminar flow of incompressible fluids in OPPCs and OTCs, respectively, the mean linear velocity is related as follows to pressure drop, Δp, column length, L, and viscosity, η[13]

$$\langle v \rangle = w^2 \Delta p / 12 \eta L \tag{15}$$

$$\langle v \rangle = d_c^2 \Delta p / 32 \eta L \tag{16}$$

These equations show that the pressure drop in an OPPC is only three-eights that in an OTC of the same critical dimensions ($w = d_c$) providing flow velocity, length, and viscosity are equal. This disadvantage of the OTC has its roots in the same geometrical factor that provided an advantage with respect to mass transfer: the encircling wall of the OTC provides greater fluid drag than the more open structure of the OPPC. The above comparisons show that OPPCs and OTCs are roughly comparable in intrinsic column efficiency, speed, and permeability. The advantages that accrue to one over another are relatively small, representing a factor of slightly under three at most. This analysis justifies our earlier emphasis that the primary advantage of the OPPC is its considerably larger volume for equal dimensions, as illustrated by eqn. 3. If we properly account for dead volume limitations, this volume gain translates into a

considerable chromatographic advantage. This gain is best illustrated by extending the treatment of Knox and Gilbert[10] to OPPC systems.

Optimization with detector volume limitations

Knox and Gilbert[10] have derived equations for optimal conditions in packed and capillary column LC based on the restraint noted earlier that detector cell volume V_c should not exceed one-half of the volume-based standard deviation σ_v of an emerging peak. They applied this criterion specifically to the non-retained peak. Considering the conflict of the very small diameter (often submicron) of chromatographically optimized OTCs, the consequent miniscule volume of the σ_v's, and the finite V_c's available or even seriously considered for detectors, the Knox–Gilbert criterion forces a many-fold increase in diameter, which in turn leads to a considerable degradation of column performance. Here we apply the Knox–Gilbert criterion to OPPC systems with the intuitive expectation that the larger volume will allow one to stay much closer to optimal chromatographic conditions and therefore suffer much less degradation in column performance.

For an OTC, Knox and Gilbert have expressed σ_v for a non-retained peak as the product of column volume and $N^{-1/2}$

$$\sigma_v(\text{OTC}) = \pi d_c^2 L/4N^{1/2} \tag{17}$$

For an OPPC this becomes

$$\sigma_v(\text{OPPC}) = waL/N^{1/2} = \alpha w^2 L/N^{1/2} \tag{18}$$

The ratio of σ_v's for the two systems when each is generating the same number N of theoretical plates is therefore

$$\frac{\sigma_v(\text{OPPC})}{\sigma_v(\text{OTC})} = \frac{4\alpha}{\pi}\frac{L_p w^2}{L_t d_c^2} \tag{19}$$

which resembles eqn. 3. This equation shows the enormous potential role of aspect ratio α in increasing σ_v to satisfy the Knox–Gilbert criterion.

Knox and Gilbert derived their detector-limited optima for OTCs using the reasonable assumption that non-equilibrium mass transport in the mobile phase is the predominant source of band broadening in the column, an assumption which is expressed by eqn. 10. They derived optimal column diameters, reduced plate heights, void times, and column lengths as a function of the allowed peak standard deviation, σ_v. The fundamental relationships used in the derivations are eqns. 1, 8, 9, 10 and 11 of their work[10]. The same relationships apply directly to the OPPC system if we substitute w for d_c.

The optimal conditions obtained by Knox and Gilbert are expressed by eqns. 23–26 of their work[10] and are cited below for comparison.

$$h = \frac{1}{\sqrt{N}}\left(\frac{16\sigma_v^2 \Delta p^3 C^3}{\pi^2 \varphi^3 \eta^3 D_m^3}\right)^{1/8} \tag{20}$$

TABLE 1

COMPARISON OF OPTIMAL PARAMETERS FOR OTC AND OPPC SYSTEMS

We have used $\eta_s = 10^{-2}$ poise and $D_m = 10^{-5}$ cm^2/sec.

σ_v / Δ_p	N	*OTCs*				*OPPCs*			
		h	t *(sec)*	d_c *(μm)*	L *(m)*	h	t *(sec)*	w *(μm)*	L *(m)*
10^{-3} μl	10000	6.97	15.6		0.852	0.680	0.0553		5.17×10^{-3}
100 bar	30000	4.03	46.8		1.48	0.392	0.166		8.95×10^{-3}
	100000	2.21	156	12.2	2.69	0.215	0.553	0.762	0.0163
	300000	1.27	468		4.67	0.124	1.66		0.0283
	1000000	0.696	1560		8.52	6.80×10^{-3}	5.53		0.0517
10^{-1} μl	10000	22.0	156		8.52	3.15	1.19		0.111
100 bar	30000	12.7	468		14.8	1.82	3.58		0.193
	100000	6.96	1560	38.6	26.9	1.00	11.9	3.53	0.351
	300000	4.02	4680		46.7	0.576	35.7		0.608
	1000000	2.20	15600		85.2	0.316	119		1.11
1 μl	10000	39.2	493		26.9	6.79	5.53		0.515
100 bar	30000	22.7	1480		46.7	3.92	16.6		0.896
	100000	12.4	4930	68.6	85.2	2.15	55.3	7.61	1.63
	300000	7.16	1.48×10^4		148	1.24	166		2.83
	1000000	3.92	4.93×10^4		269	0.680	553		5.17
10^{-3} μl	10000	16.5	8.77		1.52	1.46	0.0257		0.00759
10^3 bar	30000	9.53	26.3		2.62	0.843	0.0771		0.0131
	100000	5.22	87.7	9.15	4.79	0.462	0.257	0.519	0.0239
	300000	3.01	263		8.30	0.267	0.770		0.0415
	1000000	1.66	877		15.2	0.146	2.57		0.0759
10^{-1} μl	10000	52.3	87.7		15.2	6.79	0.553		0.163
10^3 bar	30000	30.2	263		26.2	3.90	1.66		0.283
	100000	16.6	877	29.0	47.9	2.15	5.53	2.40	0.515
	300000	9.55	2630		83.0	1.24	16.6		0.900
	1000000	5.25	8770		151	0.680	55.3		1.64
1 μl	10000	92.9	277		47.9	14.6	2.57		0.756
10^3 bar	30000	53.7	832		83.0	8.45	7.71		1.32
	100000	29.5	2770	51.4	151	4.63	25.7	5.18	2.39
	300000	17.0	8320		262	2.67	77.8		4.15
	1000000	9.33	2.77×10^4		479	1.47	257		7.59

$$t = N\left(\frac{16\varphi\eta\sigma_v^2 C^3}{\pi^2 \Delta p D_m^3}\right)^{1/4} \tag{21}$$

$$d_c = \left(\frac{16\varphi\eta D_m \sigma_v^2}{\pi^2 C \Delta p}\right)^{1/8} \tag{22}$$

$$L = \sqrt{N}\left(\frac{16\sigma_v^2 C \Delta p}{\pi^2 \varphi \eta D_m}\right)^{1/4} \tag{23}$$

The equivalent open channel relationships are derived in an identical manner and are

$$h = \frac{1}{\sqrt{N}}\left(\frac{C\Delta p\sigma_v}{\varphi\eta D_m a}\right)^{1/3} \tag{24}$$

$$t = N\left(\frac{\sigma_v^2 C^2 \varphi\eta}{\Delta p D_m^2 a^2}\right)^{1/3} \tag{25}$$

$$w = \left(\frac{\sigma_v^2 \varphi\eta D_m}{C\Delta p a^2}\right)^{1/6} \tag{26}$$

$$L = \sqrt{N}\left(\frac{\sigma_v^4 C \Delta p}{\eta D_m a^4 \varphi}\right)^{1/6} \tag{27}$$

In these relationships, t is the void elution time, C is the reduced void peak non-equilibrium coefficient ($= C_m D_m/w^2$ for OPPCs and $= C_m D_m/d_c^2$ for OTCs), and φ is the column flow resistance factor, a constant characteristic of the channel geometry equal to 32 for the OTC and 12 for the OPPC. The other terms have been previously defined.

The ratio of eqn. 21 to eqn. 25, which expresses the factor by which OTC analysis time is greater than OPPC analysis time (or, equivalently, the speed of OPPC relative to OTC), can be formulated as

$$\frac{t(\text{OTC})}{t(\text{OPPC})} = 1.172\left(\frac{\Delta p\ C_t\ a^8}{\eta\sigma_v^2 D_m \kappa^8}\right)^{1/12} \tag{28}$$

in which C_t is the Knox–Gilbert reduced mass transfer coefficient for the OTC. This equation shows that the time ratio is quite sensitive to OPPC channel breadth, a, but is not very sensitive to Δp, η, or even σ_v.

Table I is a comparison of the optimal parameters calculated from these equations as a function of σ_v, which is constrained by detector volume. Comparisons are made using the two values for σ_v cited by Knox and Gilbert, $1 \cdot 10^{-3}$ and 0.1 μl, as well as the value 1 μl. The final σ_v can be measured without undue band broadening with currently available low-volume detectors. Guiochon[14] has criticized the use of a 100-bar pressure drop in a theoretical comparison to packed columns. His criticism

points out that a small pressure drop unrealistically favors the more permeable open tubular geometry over the packed column. A pressure drop of 100 bar is perhaps not an unreasonable comparison value between the two highly permeable geometries, but for completeness, a comparison at 1000 bar is also made.

In their computations, Knox and Gilbert used the value $C = 0.08$, which corresponds to $k' = 3$. In our comparisons, we will work with void peaks exclusively. Multiplication by $(1 + k')$ may be made to examine the retained solutes which follow. Thus we use $C = 1/96$ for the OTC geometry and $C = 1/105$ for the OPPC system. Values of viscosity and diffusion coefficient are transferred directly from the Knox and Gilbert work. The channel breadth is taken as 1 in. (25.4 mm), which is a value often used successfully in our laboratory for field flow fractionation.

An examination of the data in Table I reveals that dramatic reductions in column length, reduced plate height, and void peak time may be achieved with OPPC systems relative to the OTC geometry for a given peak volume. In particular, OPPC systems of approximately 1 m length should yield $1 \cdot 10^6$ theoretical plates in 2 min (void peak time) for a peak volume of 0.1 μl with a total pressure drop of 100 bar. In general, the void peak times for OPPCs in Table I are 100–300 times shorter than those for OTCs. The short OPPC analysis time constitutes a tradeoff in technical feasibility because a convenient spacer less than 13 μm (0.0005 in.) is not readily available. However, the optimal channel thickness, w, is less than 8 μm for all cases examined. The magnitude of the optimized thicknesses, and the subsequent large pressures required for carrier flow, may furthermore demand care in the clamping of the channel to prevent leaks, and materials other than glass may be warranted. Nevertheless, the trend of the results suggests that vast improvements over the OTC may be obtained in careful work with narrow spacers.

To achieve peak volumes of 1 μl and less, one must inject a very narrow and even plug along the direction of migration. This restriction may pose great technical difficulties, but the magnitude of the results tabulated suggests the effort would be well spent to solve this problem.

EXPERIMENTAL

Equipment

Two types of OPPCs were used in the experiments. First, an uncoated channel was used to conduct plate height studies on non-retained species. Second, a column with octadecylsilane-coated walls was used to perform separations as well as to study plate height as a function of velocity for retained samples.

Uncoated channel

Construction of this column employed two glass plates, 50 mm wide, 350 mm long, and 12.7 mm thick. The channel was cut from a spacer subsequently inserted between the two plates. For the 100-μm-, 78-μm-, and 56-μm-thick channels, PTFE tape was used as the spacer. The 13-μm-thick channel was formed with a Mylar membrane spacer coated with a thin film of high vacuum grease to promote sealing. The channel cut from the spacer was 20 mm in breadth and 302 mm long and was tapered to a 30° angle at each end. A general configuration is shown in Fig. 3. Channel specifications are summarized in Table II. Stainless-steel tubing cemented in

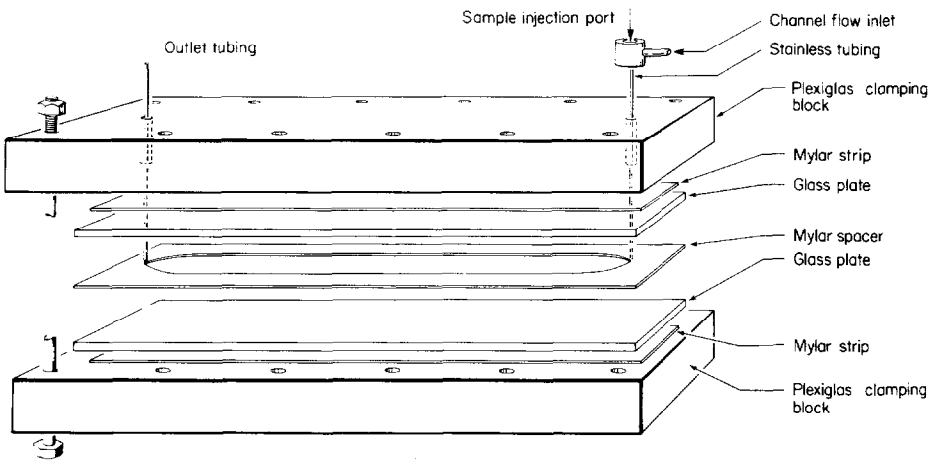

Fig. 3. Sandwich column construction typical of FFF systems, adapted for use as an OPPC chromatographic system.

1/16-in. (1.59-mm) holes in the upper glass plate constituted the channel inlet and outlet. The inlet tubing was 0.015 in. (0.381 mm) I.D. and 0.063 in. (1.600 mm) O.D. The outlet tubing for the thicker channels, 1/16 in. (1.59 mm) O.D. and 0.006 in. (0.152 mm) I.D., contained a 0.005-in. (0.127 mm) stainless-steel wire to decrease the dead volume. For the 13-μm channel, the outlet tubing was a 120-mm-long quartz capillary tube, 250 μm O.D. and 60 μm I.D.

The glass plates with their inserted spacer were sandwiched between two 390 mm × 105 mm × 50 mm Plexiglas clamping blocks. A Mylar strip (0.5 mm thick) cut to the dimensions of the channel spacer and coated with high vacuum grease was placed between the glass plates and each clamping block to distribute the pressure uniformly upon clamping. The system was clamped with sixteen evenly spaced 1/4 in. (6.35 mm) bolts (Fig. 3). Each bolt was tightened to 50–60 in. lb. of torque.

Octadecylsilane-coated channel

The glass plates in this case were prepared for coating by grinding against each

TABLE II

SUMMARY OF COLUMNS EMPLOYED IN THIS STUDY

All channels were 302 mm long with tapered ends and 20 mm in breadth.

Column No.	*Column type*	*Spacer*	*Aspect ratio, α*	*Volume (μl)*
1	Uncoated glass	100-μm PTFE tape	200	604
2	Uncoated glass	78-μm PTFE tape	256	471
3	Uncoated glass	56-μm PTFE tape	357	338
4	Uncoated glass	13-μm Mylar	1540	78.5
5	Octadecylsilane-coated	100-μm PTFE tape	200	604
6	Octadecylsilane-coated	56-μm PTFE tape	357	338
7	Octadecylsilane-coated	13-μm Mylar	1540	78.5

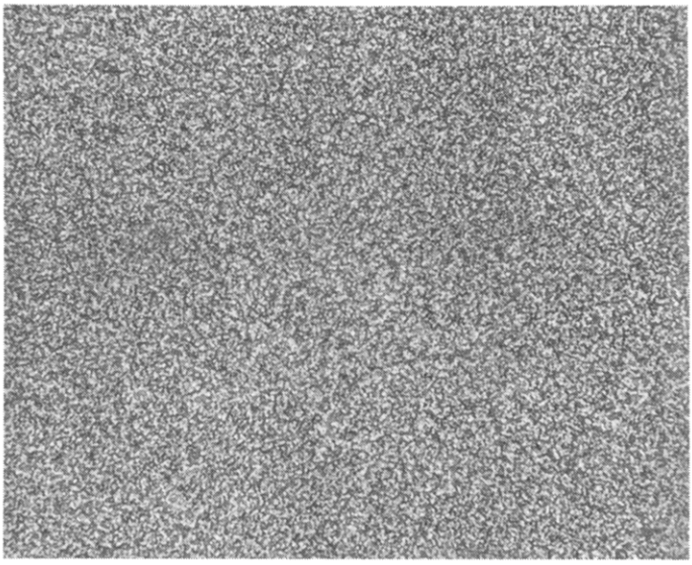

Fig. 4. Photomicrograph of ground glass surface prior to coating.

other using a grinding paste of No. 1000 silicon carbide powder in glycerin–water (1:2). Fig. 4 shows the glass surface prepared by this procedure. Following the grinding, the glass plates were thoroughly cleaned with Micro detergent (International Products, Trenton, NJ, U.S.A.), tap water, and finally distilled water. They were then immersed in an 80°C solution of 3 *M* hydrochloric acid for 5 h to effect hydrolysis of surface silica to silanol groups. The activated plates were washed with distilled water until they were neutral and were then dried at 120°C overnight.

The spacer (100 μm, 56 μm, or 13 μm thick) was sandwiched between the activated plates. The inlet and outlet had been affixed as described above. The system was clamped with binder type paper clips. The column was dried overnight in a 120°C oven with dried nitrogen continuously passed through the channel.

A 40-ml portion of a 25% (v/v) octadecyltrichlorosilane solution in toluene (pretreated with Type 4A molecular sieve) was pumped through the column at a flow-rate of 0.2 ml/min while the temperature was maintained at 100°C. Dried toluene (40 ml) was then passed through the column at a rate of 1 ml/min in order to remove the unreacted modifier from the wall surface. Then 40 ml of a 10% (v/v) water in acetonitrile mixture were used to hydrolyze the silicon–chlorine bonds. The column was again dried under nitrogen flow at 120°C overnight. To obtain maximal surface coverage by organic groups, the reacted surface was "capped" by reaction with trimethylchlorosilane in a procedure similar to that described above. Before use, the column was equilibrated by passage of a 30-ml portion of the carrier solvent to be used in the particular experiment.

Auxiliary equipment

Carrier was pumped into the column at a constant rate using a Waters Model 6000A pulse-free pump (Waters Assoc., Milford, MA, U.S.A.). A 10-μl Hamilton microsyringe was used to inject samples onto the column.

An Altex Model 153 single-wavelength (254 nm) detector (Altex, Berkeley, CA, U.S.A.) with two types of flow cells was used in this work. The effluent of the 100-μm-thick column was detected using an 8-μl commercial cell with a 100-mm-long PTFE inlet tubing of 0.012 in. (0.305 mm) I.D. into which a 0.010-in. (0.254 mm) stainless-steel wire had been inserted to decrease the dead volume.

A micro-capillary flow cell constructed in our laboratory was used for detection of effluent of the thinner columns. The design of the flow cell was suggested by Dr. Frank Yang of Varian Instruments[15]. The flow cell was made from a 12-mm length of quartz tubing of 360 μm O.D. and 220 μm I.D. The cell volume was 0.46 μl. A quartz tube of the same size was used for the reference cell. The inlet and outlet tubings of the microflow cell consisted of 100-mm lengths of 250 μm O.D., 60 μm I.D. quartz tubing connected to the flow cell with PTFE tubing. The sample and reference cells were fixed on the cell holder using an aluminum cover with screws. The light-in slit width on the holder was 0.254 μm; the light-out slit width on the cover was 1016 μm. This system permitted usage of the detector's highest sensitivity, 0.005 absorbance units/full scale deflection with a noise level of only 1%.

Chromatograms were traced on a SE-120 recorder (BBC-Metranwatt/Goerz, Edison, NJ, U.S.A.). All samples and solvents used in this work were reagent grade and chromatographic grade, respectively.

Experimental procedures

The aim of the first experiment was the verification of the expression for the velocity dependence of plate height, H, for non-retained species. The species and solvent chosen were *m*-aminobenzoic acid in the eluent, water, for which $D_m = 7.74 \cdot 10^{-6}$ cm^2/sec at 25°C[16]. The uncoated glass channel of thickness 78 μm was used to study the *H versus* velocity relationship for mean linear velocities $\langle v \rangle$ ranging from 0.2 to 3.8 mm/sec. The detector volume was 8 μl; the volume of the connecting tubing was 12 μl. The slope of the *H versus* $\langle v \rangle$ curve was compared to the value of C_m calculated from eqn. 11 with $R = 1$.

The subject of the second experiment was the study of the relationship between channel thickness and plate height. Sodium benzoate (1.66 μg/μl) in 10% (v/v) acetonitrile–water, for which we assume $D_m = 6 \cdot 10^{-6}$ cm^2/sec (based on the estimation of 10^{-5} cm^2/sec for benzoic acid[17,18]) was selected as the non-retained species. Data for *H versus* $\langle v \rangle$ curves were collected from the octadecylsilane-coated channels of thicknesses 100 μm, 56 μm, and 13 μm. Mean linear velocities ranged from 0.2 to 11.0 mm/sec. The C_m value for each channel thickness was calculated using eqn. 11 and compared to the slope of the corresponding experimental *H versus* $\langle v \rangle$ curve.

Plate height and retention characteristics of retained samples were the focus of the third experiment. A 10% (v/v) acetonitrile–water carrier solution and a sample containing benzene (0.25%), naphthalene (0.2%), and biphenyl (0.05%) were studied in the 56-μm octadecylsilane-coated column. The linear velocity $\langle v \rangle$ of the 10% (v/v) acetonitrile in water eluent varied from 0.1 to 7.8 mm/sec. Samples (0.4–0.6 μl) of the solution were injected at the various linear velocities. A plot of *H versus* $\langle v \rangle$ was obtained for each solute; the slope was again compared to the C_m value calculated from eqn. 11. A series of three sample solutions containing 0.18% sodium benzoate (non-retained), 0.2% naphthalene, and 0.2% biphenyl, respectively, was subjected to a similar procedure in the 100-μm octadecylsilane-coated column.

An expected characteristic of the OPPC column is its large sample loading capacity. The aim of the fourth experiment was to identify the onset of sample overload and to determine the effect of sample load on H for the retained species benzene, naphthalene, and biphenyl. For the overload experiment, the eluent was 10% (v/v) acetonitrile in water; the linear velocity was 5.2 mm/sec. Samples of benzene, naphthalene, or biphenyl varying in weight from 0.1 to 10 μg (100 μg for benzene) in 0.6 μl of solution were successively introduced into the 56-μm octadecylsilane-coated column. The plate height, H, was plotted as a function of sample weight for each species.

The *H versus* sample injection volume experiment was carried out in the 56 μm octadecylsilane-coated column using 10% (v/v) acetonitrile in water as the eluent with $\langle v \rangle = 2.28$ mm/sec. Either naphthalene or biphenyl, in concentrations from 0.4 to 4.0 μg/μl, was introduced into the column in 0.25–2.00-μl aliquots. The plate height was plotted as a function of sample volume for each species.

Finally, a fractogram of a solution of aromatic compounds containing 0.2% benzene, 0.1% naphthalene, 0.05% biphenyl, 0.05% anthracene, and sodium benzoate as the non-retained marker was obtained using the 13-μm-thick octadecylsilane-coated column. The eluent was 25% (v/v) acetonitrile in water, the linear velocity was 5.0 mm/sec, and the sample volume was 0.5 μl.

RESULTS AND DISCUSSION

A major effort was made in this study to measure plate heights under various conditions. Because the non-equilibrium plate height terms are rigorously calculable, departures from the theoretical values can be considered as indicative of departures from the ideal column system and experimental procedures. Non-idealities may include departures from perfect channel geometry, finite dead volumes, finite injection volumes, etc. All such non-idealities are aggravated by the attempt to develop thinner channels. It is particularly important, therefore, to monitor plate height departures from the very beginning of the study of OPPC systems.

The result of the first plate height experiment, the H *versus* $\langle v \rangle$ plot for *m*-aminobenzoic acid in column 2 ($w = 78$ μm), is shown in Fig. 5. The slope at high

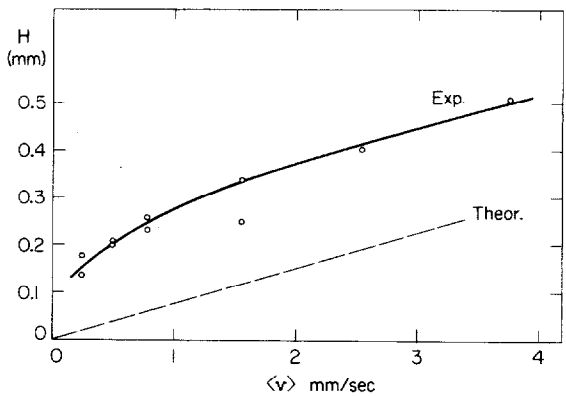

Fig. 5. Plate height, H, *versus* average linear velocity, $\langle v \rangle$, for non-retained ($R = 1$) *m*-aminobenzoic acid in water using untreated channel 2 ($w = 78$ μm).

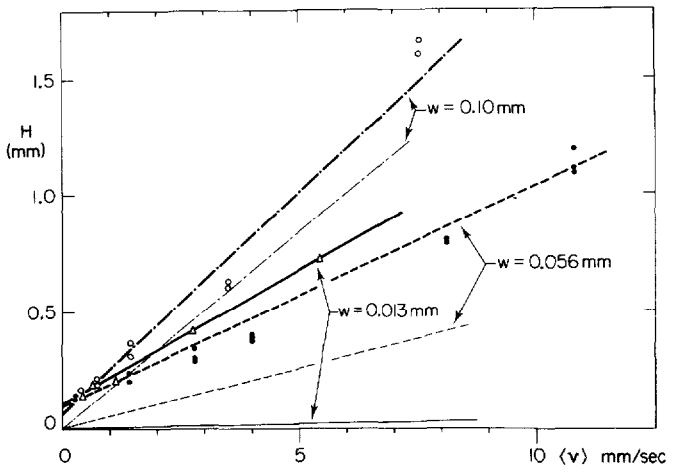

Fig. 6. Experimental (upper) and theoretical (lower) H *versus* $\langle v \rangle$ plots for non-retained sodium benzoate in OPPCs of different thicknesses, w. Mobile phase: 10% (v/v) acetonitrile in water. For calculations we use $D_m = 6 \cdot 10^{-6}$ cm^2/sec.

velocities of the experimental plot (0.075 sec) closely approximates the C_m value, 0.0748 sec, calculated from eqn. 11 using $R = 1$. However, there is a large departure in the absolute values of the plate heights, perhaps caused by dead volume effects.

For the second experiment, the H *versus* $\langle v \rangle$ plots for the non-retained sodium benzoate in the 100-μm-, 56-μm-, and 13-μm-thick octadecylsilane-coated columns (columns 5, 6 and 7, respectively) are shown in Fig. 6. The upper lines correspond to experiment for a given channel width; the lower lines are theoretical plots which are the results of substituting the D_m value cited earlier and the w values into eqn. 11 with $R = 1$. The comparison of slopes of the experimental and theoretical lines, *i.e.*, the mass transfer coefficients C_m, for each channel thickness is shown in Table III.

Fig. 6 clearly shows that for all channel thicknesses, experimental H values are greater than theoretical ones. However, for the 100-μm- and 56-μm-thick channels, the experimental slopes for the H *versus* $\langle v \rangle$ plots roughly approximate the theoretical slopes, in accord with similar results in the literature for OTCs[1]. Only in the 13-μm-thick channel does the experimental slope C_m differ markedly from the theoretical value.

TABLE III

COMPARISON OF EXPERIMENTAL AND THEORETICAL MASS TRANSFER COEFFICIENTS FOR NON-RETAINED ($R = 1$) SODIUM BENZOATE IN SEVERAL COLUMNS

Column No.	*Channel thickness, w (μm)*	C_m		$\frac{C_m \text{ expt}}{C_m \text{ theory}}$
		Expt	*Theory*	
5	100	0.190	0.167	1.14
6	56	0.094	0.052	1.80
7	13	0.114	0.003	40.5

The substantial difference between experimental and theoretical C_m values in the 13-μm channel is somewhat puzzling. The dead volume of the system, including the detector volume, was minimized to less than 1 μl. While this cannot be considered entirely negligible for so small a column volume (78.5 μl), it is not expected to contribute the large departures noted. Another possible difficulty is also related to the small channel thickness. In such a channel, any deviation from the ideal parallel plate geometry caused by, for example, inhomogeneity of the glass surface before coating, becomes a significant cause of zone deformation.

The *H versus* $\langle v \rangle$ plots of Fig. 6 would be expected to pass through (or very close to) the origin. Their failure to do so is probably the result of imperfections in the injection procedure. This seems to effect all columns equally, as suggested by the comparable intercepts.

Retained components are expected to exhibit several differences in behavior relative to non-retained substances. First, we note that the plate height in OPPC systems increases markedly with retention. The increase is over twice as large as that for OTCs in going from the non-retained condition, $R = 1.0$, to infinite retention, $R = 0$, as shown by Fig. 2. The magnitude of the change for different channel thicknesses w is illustrated in Fig. 7. The calculations for Fig. 7 are based on the assumed diffusion coefficient, $D_m = 5 \cdot 10^{-6}$ cm^2/sec. This plot clearly illustrates the necessity of working with small w values for the practical separation of retained components, where one would like $C_m \leqslant 0.1$ sec.

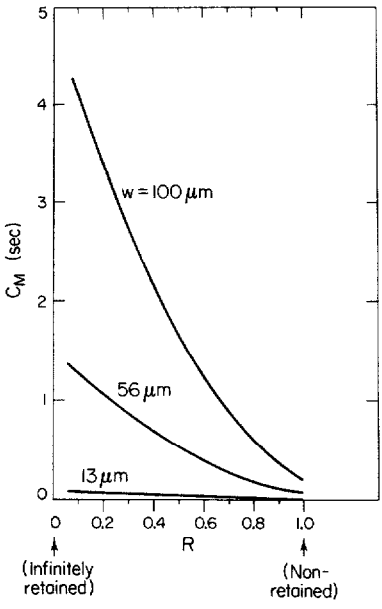

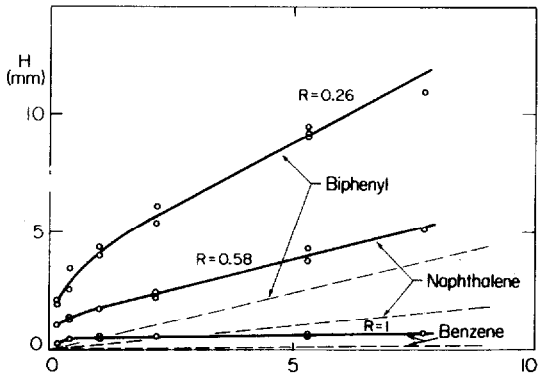

Fig. 7. Plots of C_m, calculated from eqn. 11, showing the effect of retention on plate height for OPPCs of different channel thicknesses, w. We assume $D = 5 \cdot 10^{-6}$ cm^2/sec.

Fig. 8. *H versus* $\langle v \rangle$ plots for components showing three different levels of retention in column 6, $w = 56$ μm. Mobile phase: 10% (v/v) acetonitrile in water. Diffusion coefficients are estimated via Reddy–Doraiswamy, LeBas and Perkins–Geankoplis correlations and are: benzene, $1.04 \cdot 10^{-5}$ cm^2/sec; naphthalene, $1.04 \cdot 10^{-5}$ cm^2/sec; biphenyl, $9.53 \cdot 10^{-6}$ cm^2/sec (refs. 17, 18).

The advantage of higher retention is that it increases peak volume for a given number of theoretical plates and thus tends to override the effect of extraneous dead volumes. However, we note that if plate height departures are caused by channel imperfections, retained components will show as much plate height deteriorations as non-retained components. In fact, if the imperfection is a consequence of local variations in channel thickness, w, retained components will behave worse because in the regions with larger w they will not only be carried faster by the increased flow-rate, but they will also be retained less as a consequence of the reduced relative surface area of eqn. 6.

It would require a far more comprehensive study than the present one to identify experimentally and quantitatively relate all of these effects. However, the prediction that plate height increases significantly with retention is borne out by Fig. 8, which shows H *versus* $\langle v \rangle$ plots for three retained components in column 6, $w = 56$ μm. Solid lines correspond to experiment; dashed lines correspond to theory.

Fig. 9 shows part of the results of the sample load study of the fourth experiment. In column 6 (56 μm), overloading begins at 1.5 μg for biphenyl, 2.0 μg for naphthalene, and 20 μg for benzene. Each value is significantly greater than that permitted in a comparable open tubular column[2]. Similarly, sample volumes 10–100 times greater than those permitted in the open tubular column were readily accommodated in the open channel column. Fig. 10 shows that a volume of 1.25 μl of a biphenyl solution can be injected without detrimental effect on H. For a naphthalene solution, a 2-μl injection produced no increase in H. These overload limits would, of course, be decreased somewhat for thinner, more efficient channels. However, the volume limits (≈ 2 μl) are comparable to the entire volume of a 1-m OTC of equal thickness, $d_c = w$. This latter comparison would be even more favorable for thinner OPPCs because of the increasing aspect ratio, α.

Finally, we proceed to results of more immediate interest. Fig. 11 shows a five-peak (including the void peak) chromatogram from column 7, $w = 13$ μm. The

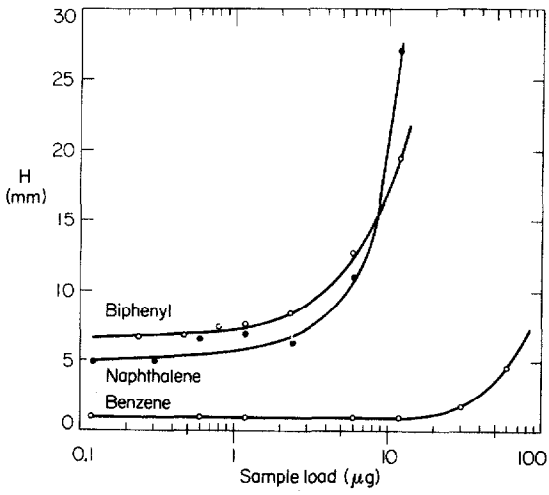

Fig. 9. Plots showing the onset of overload effects in column 6 (56 μm). Mobile phase: 10% (v/v) acetonitrile in water; $\langle v \rangle = 5.2$ mm/sec; injection volume: 0.6 μl.

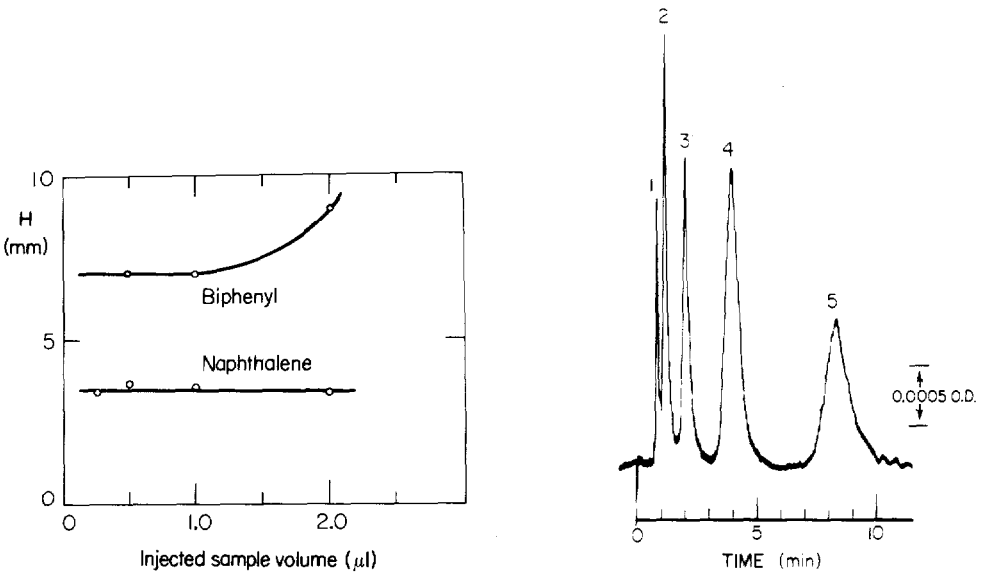

Fig. 10. Overload plots under same conditions as in Fig. 9, except sample mass is held constant at 0.8–1.0 μg and injected in a variable volume as shown on the abscissa.

Fig. 11. Separation of five aromatic components by OPPC with channel thickness, w = 13 μm (column 7). Eluent: 25% (v/v) acetonitrile in water; flow-rate = 77 μl/min; $\langle v \rangle$ = 5 mm/sec; sample volume = 0.5 μl. Components: 1 = sodium benzoate, retention time = 59 sec; 2 = benzene (0.2%), k' = 0.17; 3 = naphthalene (0.1%), k' = 1.04; 4 = biphenyl (0.05%), k' = 3.00; 5 = anthracene (0.05%), k' = 7.44.

separation is essentially complete in 10 min, with the first four peaks separated in 5 min. This result shows that the OPPC–FFF system is viable, although, of course, subject to much additional improvement.

In order to ascertain if the separation of Fig. 11 was anywhere near the potential limit for 13-μm columns, we have compared measured and theoretical values of plate height for the last three components of the figure.

The theoretical values were calculated from eqns. 10 and 11 using diffusion coefficients estimated by the method of Reddy and Doraiswamy and supported by the methods of LeBas and of Perkins and Geankoplis[17,18]. The results are presented in Table IV. The last column of the table shows that the experimental values are 5–14 times too high, which means there is room for substantial improvement. The source of the discrepancy, however, is unclear. If the excessive experimental values stemmed

TABLE IV

COMPARISON OF CALCULATED AND THEORETICAL PLATE HEIGHTS FROM THE LAST THREE PEAKS OF FIG. 11

Peak	*R*	$D_m \times 10^{-6}$ *(cm²/sec)*	*H(calc) (mm)*	*H(exp) (mm)*	*H(exp)/H(calc)*
Naphthalene	0.49	10.	0.072	0.98	14
Biphenyl	0.25	9.4	0.138	1.06	7.7
Anthracene	0.12	9.2	0.179	0.94	5.3

from dead volume effects, we would expect the measured plate height to decrease significantly through the series of peaks. This is clearly not so, especially when we consider that the void peak mentioned earlier yielded $H \approx 0.6$ mm at the same flow-rate. More likely the effect is due to channel imperfections, but there may be some fractional contribution of dead volume effects.

CONCLUSIONS

The preliminary results discussed above, particularly the fractogram, show that OPPC systems based on the FFF sandwich-like construction provide a promising approach to realize the advantages of capillary LC without the accompanying disadvantage of low column volumes. Additional work is required to push channel thickness to lower values while maintaining the integrity of the channel flow space. One should not have serious volumetric problems, even at just a few micrometers thickness, providing channel breadth can be maintained at 1–2 cm.

A critical evaluation of the present work suggests several amendments and extensions that should make the overall method even more effective. For example, the theory does not account for fluid drag at the edges, which retards the zone in the edge regions, leading to some zone distortion and tailing. The effect is probably not of major importance for large aspect ratios and fast elution because the flow distortion will only extend into the channel for a few spacer widths, and its effects are abetted by a diffusion distance approximately equal to $(D_m t)^{1/2}$. The latter is only a fraction of a millimeter for almost all void peak times expressed in Table I. One could avoid edge difficulties by injecting the sample in the center of the channel downstream from the flow inlet. Such a strategy has been used in FFF[19]. One could also introduce streams of carrier flow near the edges to serve as a sheath which would exclude the solute from any desired portion of the edge regions.

In a similar way, the triangular ends of the channel cause some zone curvature and distortion. A non-equilibrium contribution to plate height will arise due to the inequalities in the distance the zone must travel before it exits the channel. One could circumvent this by several modifications, the most simple of which would entail using a much thinner channel over the specific area covered by the triangles.

Novotny *et al.*[20] have shown considerable promise for capillary chromatography using supercritical fluids. The more rapid diffusivity of supercritical fluids, relative to confentional LC solvents, allows one to use a wider bore without sacrifices in separation time. Nonetheless, it is likely that OPPCs would provide more flexibility in mutually adjusting sample size, flow-rate, and pressure drop to desirable levels.

Finally, some way might eventually be found to profitably combine FFF and LC. In this combination, the lateral field of FFF could be imagined to have two roles. Most obviously, the lateral field, combined with differential flow, would contribute to separation, as is expected of FFF[5–7]. Additionally, however, the lateral field might be used to form extremely thin solute layers so that mass transfer would be exceedingly fast. This could perhaps be accomplished in columns of moderately wide bore where mass transfer would normally be slow. With such favorable dynamics stemming from the application of the field, one could then rely partially, or perhaps principally, on the chromatographic process to provide the specific kind of selectivity needed for separation.

ACKNOWLEDGEMENTS

The authors wish to acknowledge the help of Dr. Frank Yang with the low-volume detection system.

This investigation was supported by Public Health Service Grant GM 10851-25 from the National Institutes of Health.

SYMBOLS

a	column breadth (mm)
C	dimensionless non-equilibrium coefficient of the Knox–Gilbert analysis
C_m	general non-equilibrium coefficient (sec)
C_t	dimensionless non-equilibrium coefficient for the OTC
d_c	open tubular capillary diameter (μm)
D_m	solute diffusion coefficient in the mobile phase (cm^2/sec)
$f_p(R)$	parabolic retention function for parallel plate system
$f_t(R)$	parabolic retention function for open tubular columns
h	reduced plate height
H	plate height (mm)
k'	capacity factor; g solute in stationary phase/g solute in mobile phase
K'	equilibrium distribution ratio; g solute per mm^2 stationary phase/g solute per mm^3 mobile phase
L	column length (m)
L_p	column length of OPPC (m)
L_t	column length of OTC (m)
N	theoretical plate number
OPPC	open parallel plate column
OTC	open tubular column
Δp	pressure drop (bar)
R	retention ratio
S/V	surface area to volume column ratio (mm^{-1})
t	void time elution (sec)
t_p	void time elution for OPPC (sec)
t_t	void time elution for OTC (sec)
$\langle v \rangle$	average mobile phase linear velocity (mm/sec)
V_c	detector cell volume (μl)
V^0	column void volume (μl)
V_r	retention volume of analyte (μl)
w	channel thickness (μm)
α	aspect ratio, a/w
η	solvent viscosity (poise)
κ	plate height efficiency ratio, $f_p(R)/f_t(R)$
σ_v	standard deviation of a peak in volume units (μl)
φ	flow resistance parameter

REFERENCES

1 T. Tsuda and M. Novotny, *Anal. Chem.*, 50 (1978) 632.
2 T. Tsuda, K. Hibi, I. Nakanishi, T. Takeuchi and D. Ishii, *J. Chromatogr.*, 158 (1978) 227.
3 R. Tijssen, J. P. A. Bleumer, A. L. C. Smit and M. E. van Kreveld, *J. Chromatogr.*, 218 (1981) 137.
4 M. Krejčí, K. Tesařík, M. Rusek and J. Pajurek, *J. Chromatogr.*, 218 (1981) 167.
5 E. Grushka, K. D. Caldwell, M. N. Myers and J. C. Giddings, *Separ. Purif. Methods*, 2 (1973) 127.
6 J. C. Giddings, M. N. Myers, K. D. Caldwell and S. R. Fisher, in D. Glick (Editor), *Methods of Biochemical Analysis*, Wiley, New York, 1980, p. 79.
7 J. C. Giddings, M. N. Myers and K. D. Caldwell, *Separ. Sci. Technol.*, 16 (1981) 549.
8 J. C. Giddings, M. Martin and M. N. Myers, *J. Polymer Sci., Polymer Physics Ed.*, 19 (1981) 815.
9 J. C. Giddings, M. Martin and M. N. Myers, *J. Chromatogr.*, 158 (1978) 419.
10 J. H. Knox and M. T. Gilbert, *J. Chromatogr.*, 186 (1979) 405.
11 J. C. Giddings, *J. Chromatogr.*, 5 (1961) 46.
12 J. C. Giddings, *Dynamics of Chromatography*, Marcel Dekker, New York, 1965.
13 R. Fox and A. McDonald, *Introduction to Fluid Mechanics*, Wiley, New York, 2nd ed., 1978, pp. 338, 349.
14 G. Guiochon, *Anal. Chem.*, 53 (1981) 1318.
15 F. J. Yang, Varian Instrument Group, Walnut Creek, CA, personal communication, 1981.
16 R. C. Weast (Editor), *CRC Handbook of Chemistry and Physics*, CRC Press, Cleveland, 55th ed., 1974, p. F60.
17 T. Sherwood, R. Pigford and C. Wilke, *Mass Transfer*, McGraw-Hill, New York, 1975, pp. 26–31.
18 R. Reid, J. Prausnitz and T. Sherwood, *The Properties of Gases and Liquids*, McGraw-Hill, New York, 3rd ed., 1977, pp. 571–590.
19 L. K. Smith, M. N. Myers and J. C. Giddings, *Anal. Chem.*, 49 (1977) 1750.
20 M. Novotny, S. Springston, P. Peaden, J. Fjeldsted and M. Lee, *Anal. Chem.*, 53 (1981) 407A.